

Selective recovery of valuable metals from spent lithium-ion batteries – Process development and kinetics evaluation



Wenfang Gao ^{a, b}, Jiali Song ^{a, c}, Hongbin Cao ^{a, b, c}, Xiao Lin ^{a, b, **}, Xihua Zhang ^{a, d}, Xiaohong Zheng ^{a, b}, Yi Zhang ^{a, b, c}, Zhi Sun ^{a, b, *}

^a Beijing Engineering Research Centre of Process Pollution Control, Division of Environment Technology and Engineering, Key Laboratory of Green Process and Engineering, Institute of Process Engineering, Chinese Academy of Sciences, Beijing, 100190, China

^b University of Chinese Academy of Sciences, Beijing, 100049, China

^c National Engineering Research Center of Distillation Technology, School of Chemical Engineering and Technology, Tianjin University, Tianjin, 300072, China

^d Solid Waste and Chemicals Management Center, Ministry of Environmental Protection of China, Beijing, 100029, China

ARTICLE INFO

Article history:

Received 25 August 2017

Received in revised form

5 December 2017

Accepted 7 January 2018

Available online 10 January 2018

Keywords:

Lithium-ion battery

Selective leaching

Acetic acid

Leaching kinetics

Reducant

Li₂CO₃

ABSTRACT

Recovery of valuable metals from spent lithium-ion battery (LIB) is of both environmental and economic importance. Acidic leaching usually encounters issues of low selectivity or slow kinetics with considerable secondary waste generation during further purification. In this research, a closed-loop process with improved leaching selectivity for recycling of spent LiNi_xCoyMn_{1-x-y}O₂ battery using weak acidic leachant was demonstrated. To obtain optimal conditions of the leaching process, the effects of acid concentration, solid to liquid (S/L) ratio, temperature and reductant content were systematically investigated. Almost all Co, Li, Mn and Ni could be effectively recovered into the solution while Al remained in the residue as metallic form, after one-step leaching. The role of reductant during leaching was further evaluated which was found to be critical for the leaching kinetics. It is clear that the addition of reductant could alter the rate-controlling step of leaching from the ion diffusion in the residue layer to the surface chemical reactions. With high selectivity against impurities, this research proposed and verified a process to recover high purity Li₂CO₃ from the cathode scrap of LIBs, and more than 90% of the global recovery rate of valuable metals can be achieved.

© 2018 Elsevier Ltd. All rights reserved.

1. Introduction

Compared with lead-acid batteries and Ni-MH batteries, lithium-ion batteries (LIBs) have been widely used in cellular phones, laptop computers and recently in electric vehicles because of their outstanding electrochemical properties (Wang et al., 2016; Weng et al., 2013). The high consumption of LIBs inevitably leads to a large number of spent LIBs generation worldwide. It is reported that the quantity and weight of spent LIBs only in 2020 will reach 25 billion units and 500 thousand tons in China (Zeng et al., 2014). The recovery of spent LIBs is beneficial to resource conservation

and thus alleviation of energy crisis (Hanisch et al., 2015). Most importantly, it is also highly desirable to prevent environmental problems such as soil and groundwater contamination (Nayaka et al., 2016).

Since the cathode material is the most important and valuable component in LIBs, the recovery of cathode material has gained great attention from researchers worldwide (Yang et al., 2014). Motivated by recycling cobalt which was a critical material, numerous studies have paid close attention to the recovery of LiCoO₂ rather than other materials (e.g., LiMn₂O₄, LiNi_xCo_{1-x}O₂ and LiNi_xCoyMn_{1-x-y}O₂) in the past decade (Zhang et al., 2015). In general, there are three typical categories of technologies for the separation and recovery of metals from spent LIBs where hydrometallurgy is a kind of well-established process. Compared with pyrometallurgy and biometallurgy processes (Xin et al., 2016), hydrometallurgy can achieve higher purity, lower energy consumption and lower gas emission (Joulie et al., 2017). Acidic leaching plays a critical role in the hydrometallurgical processes which can transfer metal values from solid to aqueous solution. The

* Corresponding author. National Engineering Laboratory for Hydrometallurgical Cleaner Production Technology, Institute of Process Engineering, Chinese Academy of Sciences, No. 1 Beierjie, Zhongguancun, Haidian District, Beijing, China.

** Corresponding author. National Engineering Laboratory for Hydrometallurgical Cleaner Production Technology, Institute of Process Engineering, Chinese Academy of Sciences, No. 1 Beierjie, Zhongguancun, Haidian District, Beijing, China.

E-mail addresses: xlin@ipe.ac.cn (X. Lin), sunzhi@ipe.ac.cn (Z. Sun).

typical acids used in the leaching process include some inorganic acids such as H_2SO_4 (Gratz et al., 2014; Pagnanelli et al., 2014; Zou et al., 2013), HCl (Guo et al., 2015; Shuva and Kurny, 2013) and HNO_3 , or organic acids (e.g. citric acid (Chen et al., 2016), DL-malic acid (Yao et al., 2016) and oxalic acid (Sun and Qiu, 2012)). To improve the leaching efficiency, reductants (e.g. H_2O_2 (Li et al., 2015; Sa et al., 2015; Zou et al., 2013), glucose (Chen et al., 2016; Granata et al., 2012; Pagnanelli et al., 2014) and NaHSO_3 (Meshram et al., 2015a; Pagnanelli et al., 2014)) are often introduced to the leaching solutions to convert the higher valence metals (e.g. Co^{3+} , Mn^{4+}) to lower valence metals (e.g. Co^{2+} , Mn^{2+}). Despite high leaching efficiency for each metal can be achieved, the leaching processes by inorganic acids had a lower selectivity and might involve adverse impacts on the environment such as hazardous gases emission (e.g., Cl_2 , SO_2) and the generation of waste mineral acids (Chen et al., 2016). By contrast, the leaching processes based on organic acids are increasingly attracting the researchers' attention because of their excellent leaching efficiencies, avoiding secondary pollution and recyclable properties. Before the leaching process, the cathode material is usually separated from the aluminum foil. Various processes, such as mechanical treatment (Chen et al., 2016; Granata et al., 2012), vacuum pyrolysis (Sun and Qiu, 2012; Yao et al., 2016), thermal treatment, alkali dissolution (Pagnanelli et al., 2014) and physical dissolution (e.g. N-Methyl pyrrolidone (Yang et al., 2015)), are often adopted in the recycling processes. However, some pretreatment processes are characterized as complicated and high energy consumption, and the generated organic liquid is difficult to be recycled. Aiming to simplify the recycling process and reduce the environmental impact, a novel selective leaching process with low leaching efficiency of aluminum is critical to be considered and developed.

Closely related to the treatment capacity and cost for industrial application, the leaching kinetics can be employed to identify the interaction between unreacted particles and the leachant (Meshram et al., 2015a). It is widely acknowledged that the kinetics models mainly include layer mass transfer control model, surface chemical reaction control model (Abdel-Aal and Rashad, 2004; Aydogan et al., 2007; Dömez et al., 2009), residue layer diffusion control model (Hoşgür and Kurama, 2012) and the Avrami equation (Khawam and Flanagan, 2006). Among these models, the Avrami equation is originally developed and well verified for the kinetics of crystallization (Behera and Parhi, 2016; Li et al., 2011; Liu et al., 2014). Li et al. (2014) investigated vanadium leaching from a spent selective catalytic reduction catalyst, the leaching parameters could be described well by the Avrami equation with $-\ln(1-X) = 0.96 \times [\text{H}_2\text{SO}_4]^{0.21}(S/L)^{-0.35} e^{-5900/RT} t^{0.12}$ in which each leaching condition was analyzed. However, a few studies were performed to investigate the leaching kinetics of metal values from cathode scrap, and mainly focused on the determination of rate-limiting step and the corresponding activation energies (Jha et al., 2013; Meshram et al., 2015a). Taking other leaching parameters such as acid concentration, S/L ratio and reductant content into consideration, a comprehensive kinetics model needs to be established to quantitatively illustrate the kinetics behavior during the leaching process of metal values from the cathode scrap.

Zhang et al. (2015) developed and demonstrated a closed-loop process for recycling $\text{LiNi}_{1/3}\text{Co}_{1/3}\text{Mn}_{1/3}\text{O}_2$ from the cathode scrap of LIBs. Trichloroacetic acid (TCA) was employed as leachant to obtain a lower Al dissolution rate to recycle Al foil and leach out other metal values from the cathode scrap. The process optimization and kinetics analysis were also performed. However, TCA is more expensive than other common organic acids which may limit the industrial application, and the recycling of waste acids should be considered. Even with formic acid, the formation of precipitates

during leaching requires prudent monitoring of the leaching conditions in order to ensure high selectivity of lithium (Gao et al., 2017). Furthermore, detailed and quantitative evaluation on the leaching kinetics and the role of reductant was missing. The purpose of this research is to present a method with improved selectivity against impurities for recycling cathode scrap of spent LIBs under a weak acid while the leaching kinetics can be evaluated from the role of reductant. $\text{LiNi}_{1/3}\text{Co}_{1/3}\text{Mn}_{1/3}\text{O}_2$ based cathode scrap was chosen as a typical candidate for metal recovery. At first, by optimizing the acid concentration, ratio of cathode scrap to leaching solution (S/L), reductant content, leaching temperature and time, the maximum leaching efficiencies and highly selectivity can be achieved. In addition, taking account of acid concentration, S/L ratio and reaction temperature, the leaching kinetics and role of reductant were evaluated in detail. At the same time, through kinetics evaluation along with characterizations including SEM and XRD, new insights were offered into the quantitative influence of reductant on the leaching behavior. Finally, a new process was developed to recover high purity Li_2CO_3 from the cathode scrap of spent LIBs with high selectivity and recovery efficiency of valuable metals.

2. Experimental

2.1. Materials and reagents

Supplied by a local recycling company (Brump Recycling Co. Ltd.), the spent lithium-ion batteries were firstly discharged to avoid short-circuiting and self-ignition. They were then dismantled manually into cathode and anode, while the plastic and steel cases that cover the batteries were removed. After cutting into pieces with the size of $10 \text{ mm} \times 10 \text{ mm}$ and dried at 60°C for 24 h, the cathode scrap was dissolved in the aqua regia solution (HNO_3 : $\text{HCl} = 1:3$, v/v) to determine the composition. The mass fraction of the cathode scrap is provided as follows: 7.86% aluminum, 18.32% nickel, 18.65% cobalt, 17.57% manganese and 6.15% lithium, respectively. All chemical reagents were of analytical grade and all solutions were prepared with ultrapure water (Millipore Milli-Q).

2.2. Selective leaching of cathode scrap

The leaching experiments were carried out in batch using a 500 mL three-necked round bottom glass flask which was placed in a temperature-controlled water bath with a magnetic stirrer. The reflex condenser was connected with the glass flask to avoid the evaporating of acetic acid. A given mass of cathode scrap was added to a 250 mL aqueous solution containing acetic acid and reductant. The leaching conditions including the acetic acid concentration, S/L ratio, reductant content and reaction temperature were investigated systematically. During the leaching process, a series of liquid samples with a volume of approximate 1 mL were taken out from the leachate to get the local leaching rate of each metal for further kinetic analysis. After leaching, the leaching residues (Al foil, undissolved organic binder and conductive reagent) were vacuum filtered immediately. Dried at 80°C for 24 h, the leaching residues were sieved by a sieving mesh with the pore size of 5 mm to obtain Al foil. After being washed with ultrapure water, Al foil can be recovered with high purity. The leaching efficiency of each metal from the cathode scrap is determined as follows

$$y = \frac{C_{W,t} \times V}{m_W} \times 100\% \quad (1)$$

where y (wt.%) is the leaching rate of metal W ($W=\text{Ni}, \text{Co}, \text{Mn}, \text{Li}$,

Al , $C_{W,t}$ (g/L) is the concentration of metal W in the leachate at the leaching time of t (min), V (L) is the volume of leachant, m_W (g) is the mass of metal W in the cathode scrap.

2.3. Preparation of lithium carbonate

The pH of leachate was firstly adjusted to 6.45 by adding NaOH to remove Al^{3+} . After vacuum filtration, the pH of leachate was then adjusted and maintained at 11 for 24 h by adding NaOH and NH_4OH solutions with the pumping speed of 2 mL/min under N_2 protection at 65 °C with stirring speed of 1300 rpm. The mixture of $Co(OH)_2$, $Ni(OH)_2$ and $Mn(OH)_2$ could be fully co-precipitated. The obtained co-precipitate was washed with ultrapure water and dried at 80 °C for 24 h, and it could be used to prepare Ni-Co-Mn precursor (Zou et al., 2013). With the addition of acetic acid, the solution was adjusted to neutral. Subsequently, Li_2CO_3 was precipitated by adding saturated Na_2CO_3 solution to the raffinate at 20–60 °C. To further improve the purity of the Li_2CO_3 , it was washed with boiling ultrapure water and dried at 80 °C for 12 h. The residual solution and washing liquor were collected, evaporated and then recycled to the pH adjustment process to increase the recovery of Li.

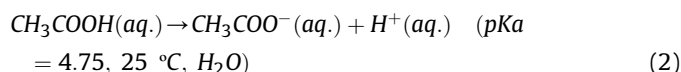
2.4. Characterizations

The crystal structures of cathode and other materials were characterized by X-ray diffractometer (X'pert PRO, PANalytical) with $Cu K\alpha$ radiation. The concentrations of Al^{3+} , Ni^{2+} , Co^{2+} , Mn^{2+} and Li^+ in solutions were measured by inductively coupled plasma optical emission spectrometer (ICP-OES, iCAP 6300, Radial, Thermo Scientific). The morphology was observed by a mineral liberation analyzer (MLA 250, FEI) which was equipped with an energy dispersive spectrometer (EDS, EDAX GenesisSiLi) and a scanning electron micrometer (SEM, Quanta 250).

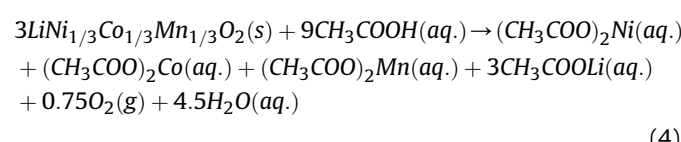
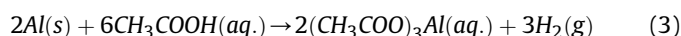
3. Results and discussion

3.1. Selective leaching of cathode scrap

The hydrometallurgical processes based on environment-friendly leachants possess many advantages such as less emission of hazardous gases, easily degradable under aerobic and anaerobic conditions, possible regeneration property (Behera and Parhi, 2016). As a typical environment-friendly and low-cost leachant, acetic acid has been found to be efficient in leaching valuable metals from lead acid battery paste components with minimal pollution and low energy consumption (Zhu et al., 2013). The acid ionization equation of acetic acid can be given as follows:



The chemical reactions during the leaching process can be described as follows:



To explore the effect of acetic acid on the leaching of metal values, two experiments were conducted under the following conditions according to the previous work (Zhang et al., 2015):

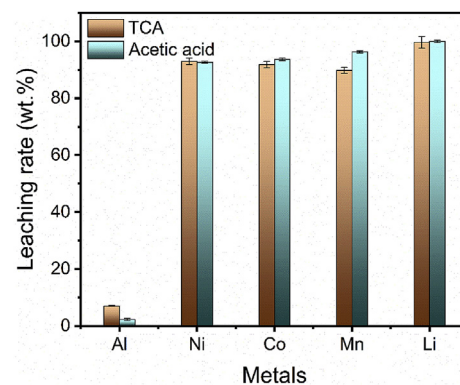


Fig. 1. Leaching rates of Al, Li, Co, Ni and Mn from the cathode scrap in TCA and acetic acid.

leachant (TCA, acetic acid) concentration of 3.0 mol/L, S/L ratio of 50 g/L, H_2O_2 content of 4 vol%, leaching at 60 °C for 30 min. The leaching rates of Al, Co, Mn, Li and Ni in TCA and acetic acid are presented in Fig. 1. For the leaching of Al, the leaching rate in acetic acid was lower than TCA, thus almost all the Al can be recovered in its metallic form. At the same time, for the leaching of Li, Ni, Co and Mn, the leaching rates in acetic acid were higher than TCA. Therefore, compared with TCA, acetic acid showed better selectively towards Al, while the leaching rates of Li, Ni, Co and Mn still maintained higher level.

3.1.1. Effect of acetic acid concentration

To investigate the effect of acetic acid concentration (1–5 mol/L) on the leaching of the cathode scrap, the experiments were performed under the following conditions: S/L ratio of 50 g/L at 60 °C. A series of samples were taken out ranging from 0 to 120 min. As shown in Fig. 2, the leaching rates of Ni, Co, Mn and Li under different acetic acid concentrations increased with the leaching time within the initial 45 min, and tended to be stable after 45 min. The leaching rates of Ni, Co, Mn and Li clearly increased with acetic acid concentration, and Li was much easily leached out than other metals (Fig. S1). When the acetic acid concentration increased to 3.5 mol/L, there was no obvious increase in the leaching rates. To guarantee the higher leaching rate and lower acid consumption, 3.5 mol/L was chosen as the optimal leachant concentration for following experiments.

3.1.2. Effect of S/L ratio

To investigate the effect of S/L ratio (30–90 g/L) on the leaching rates of metal values, experiments were conducted under the following conditions: 3.5 mol/L acetic acid, leaching at 60 °C for 0–120 min. As indicated in Fig. 3, the leaching rates of Ni, Co, Mn and Li all decreased with the S/L ratio increased from 30 g/L to 90 g/L, and there was a clear decrease from 40 g/L to 50 g/L (Fig. S2). However, the leaching rate of Al had no obvious fluctuation with the increase of S/L ratio. Considering the treatment capacity and leaching rates of metal values, the S/L ratio of 40 g/L would be employed in the following experiments.

3.1.3. Effect of reaction temperature

As an important factor, reaction temperature has a significant effect on the leaching of metal values from the cathode scrap. To study the effect of reaction temperature, experiments were performed under the following conditions: 3.5 mol/L acetic acid, S/L ratio of 40 g/L, reaction temperature ranging from 30 °C to 80 °C and leaching time from 0 min to 90 min. As shown in Fig. 4(a), the leaching rate of Al obviously increased with the increase of reaction

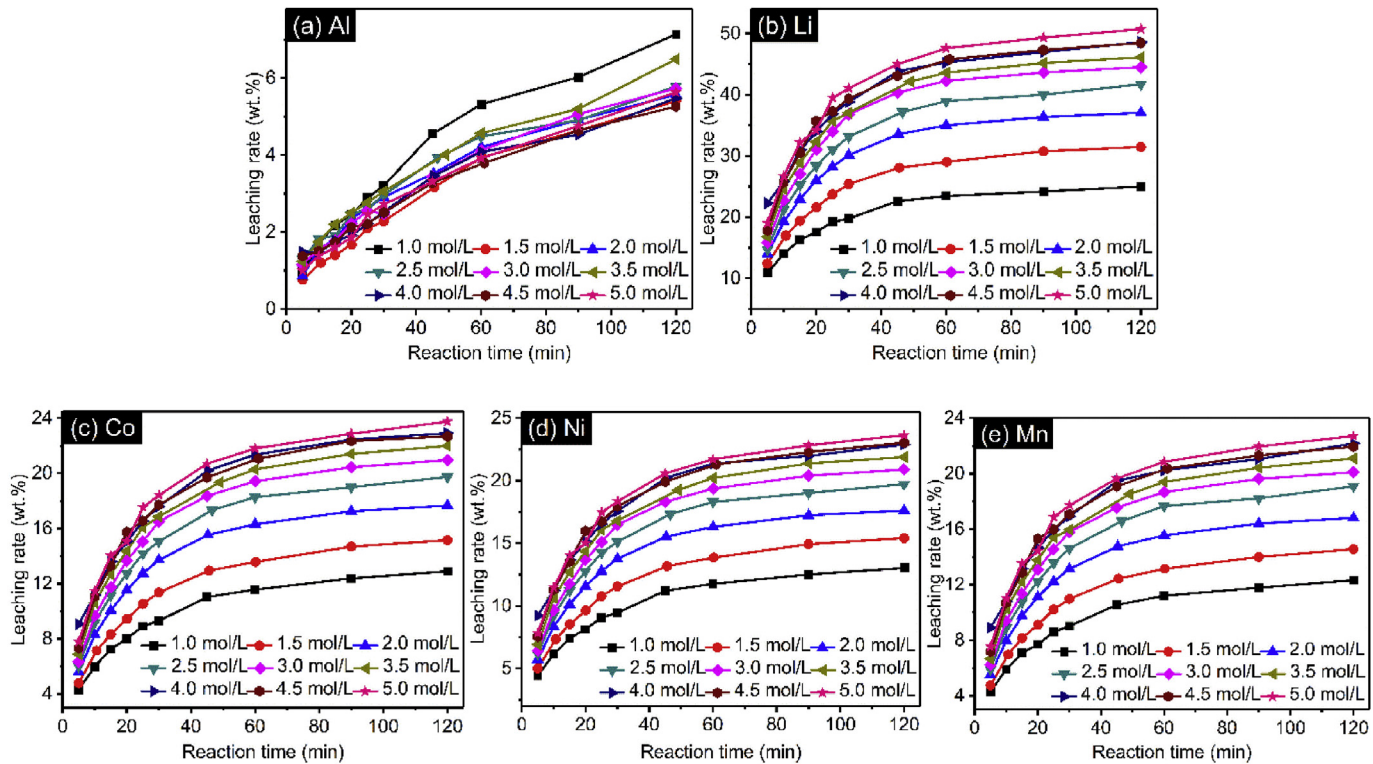


Fig. 2. Leaching rates of (a) Al, (b) Li, (c) Co, (d) Ni and (e) Mn from the cathode scrap under different acetic acid concentrations in the absence of reductant.

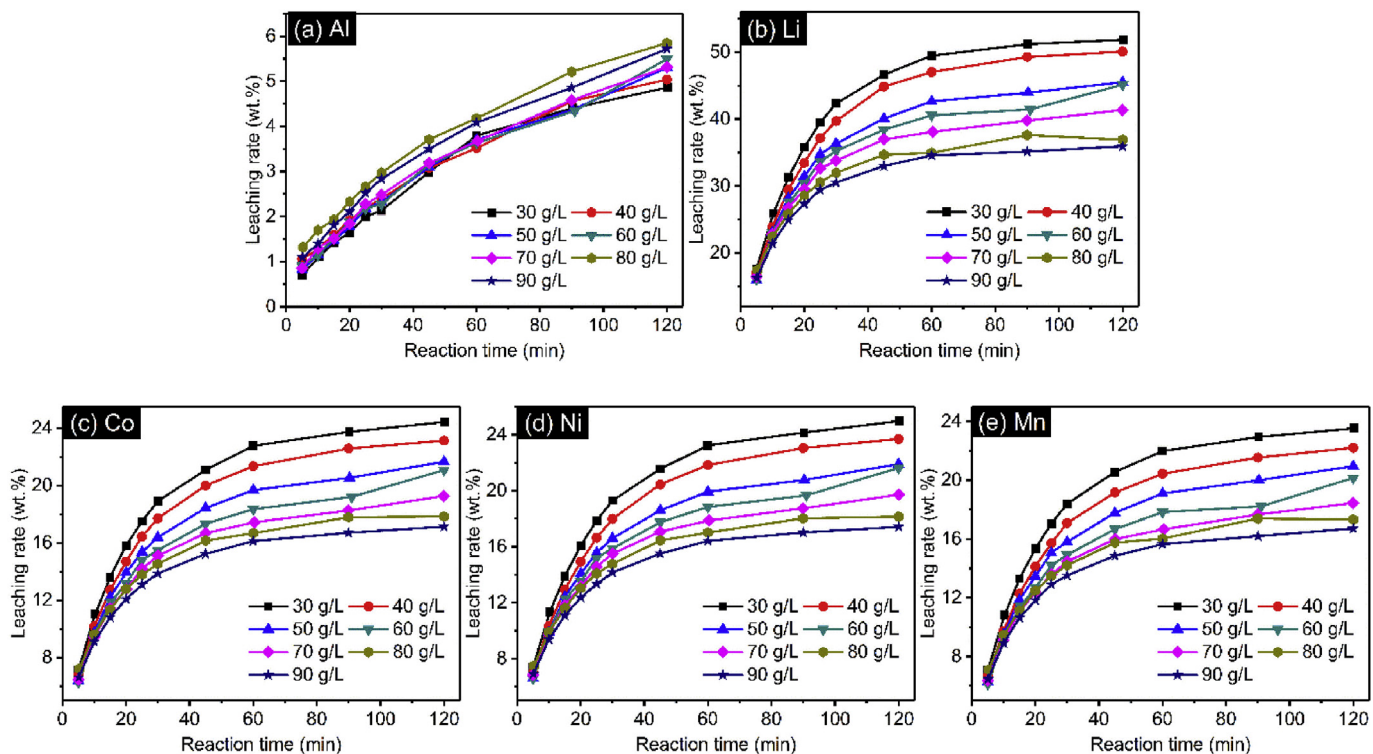


Fig. 3. Leaching rates of (a) Al, (b) Li, (c) Co, (d) Ni and (e) Mn from the cathode scrap under different S/L ratios in the absence reductant.

temperature from 30 °C to 80 °C. It is revealed that more Al would be transferred to the leachate under higher reaction temperature. The leaching rates of Li, Ni, Co and Mn showed similar trend, they

increased with the increase of reaction temperature from 30 °C to 60 °C but decreased when the reaction temperature was higher than 60 °C (Fig. 4 and Fig. S3). This finding showed that the reaction

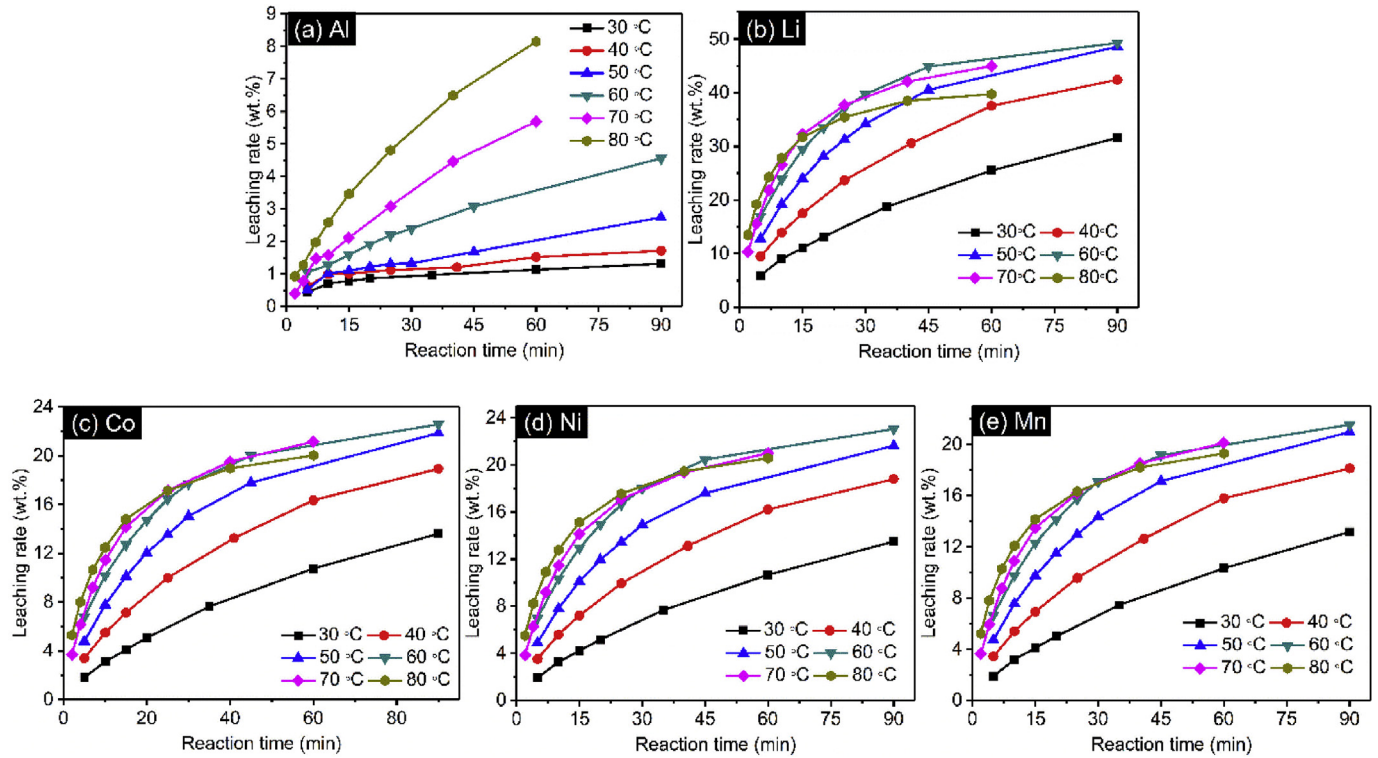
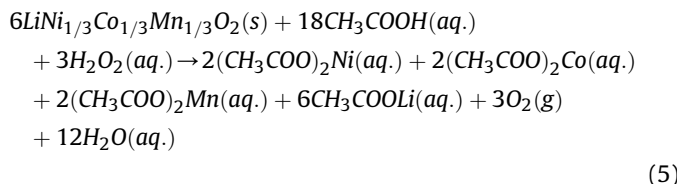


Fig. 4. Leaching rates of (a) Al, (b) Li, (c) Co, (d) Ni and (e) Mn from the cathode scrap under different reaction temperatures in the absence of reductant.

between acetic acid and $\text{LiNi}_{1/3}\text{Co}_{1/3}\text{Mn}_{1/3}\text{O}_2$ was an exothermic reaction where increasing the leaching temperature can promote the reaction speed, but the leaching process would be refrained under higher temperatures. Therefore, the optimal reaction temperature can be set at 60 °C in which the highest leaching rates of Li, Ni, Co and Mn could be achieved, but the leaching rate of Al was only 4.56 wt% at the leaching time of 90 min.

3.1.4. Effect of reductant content

Since the leaching rates of Ni, Co and Mn in cathode scrap were only around 25 wt% in the absence of reductant, it is necessary to convert more Co^{3+} and Mn^{4+} into the easily dissolved Co^{2+} and Mn^{2+} to promote the leaching process by introducing proper reductants. As no other impurity ions would be introduced to the leachate, hydrogen peroxide was selected as the reductant in this research. The reaction between acetic acid and the cathode scrap at the presence of H_2O_2 may be presented as follow:



As shown in Fig. 5, the reductant content on the leaching rates of metal values was investigated. The leaching rates of Li, Ni, Co and Mn increased from around 25 wt% to nearly 100 wt% within 25 min (Fig. 5 (b, c, d and e)), while the leaching rate of Al decreased to lower than 2 wt% (Fig. 5(a)) after the addition of H_2O_2 . With the increase of the H_2O_2 content from 0 vol% to 4 vol%, the leaching rates of Li, Ni, Co and Mn increased, and there was a platform for the leaching rates of nearly 100 wt% when the reductant content was higher than 4 vol% (Fig. S4). The leaching rates of Co, Li, Mn and Ni

could achieve 93.62 wt%, 99.97 wt%, 96.32 wt% and 92.67 wt%, respectively, while the leaching rate of Al was only 2.36 wt% when the H_2O_2 content was 4 vol%. Therefore, the optimal H_2O_2 content was chosen as 4 vol% in the subsequent experiments. Compared with the leaching results in other studies (Table 1), after a one-step leaching process, the leaching efficiency of acetic acid reached a higher leaching rate and selectivity for Ni, Co, Mn and/or Al based cathode materials.

To investigate the quantitative effect of reductant on the leaching kinetics, the leaching experiments under different reaction temperature, acid concentration and S/L ratio at the presence of H_2O_2 were also conducted, and the experimental results were presented in Figs. S5, S6 and S7.

3.2. Leaching mechanisms

To find out and verify the relationship between leaching mechanisms and the leaching parameters, kinetics analyses were carried out during the leaching process with and without H_2O_2 . Since the binder and acetylene black conductive agent can form a gray residue layer with loose and porous structure during leaching process of metal values from the cathode scrap of LIBs (Zheng et al., 2017), the leaching process can be divided into the following steps: (1) mass transfer of reactive ions through liquid film to residue-film interface, (2) diffusion from residue-film interface through the residue layer to the reaction interface, (3) chemical reaction on the surface of the particle $\text{LiNi}_{1/3}\text{Co}_{1/3}\text{Mn}_{1/3}\text{O}_2$, (4) product diffusion through the residue layer, (5) product transfer through the liquid film to the bulk solution.

The leaching process of metal values from the cathode scrap of LIBs is actually a solid-liquid-gas heterogeneous process, and the leaching kinetic can be described by the following equation (Sun et al., 2009):

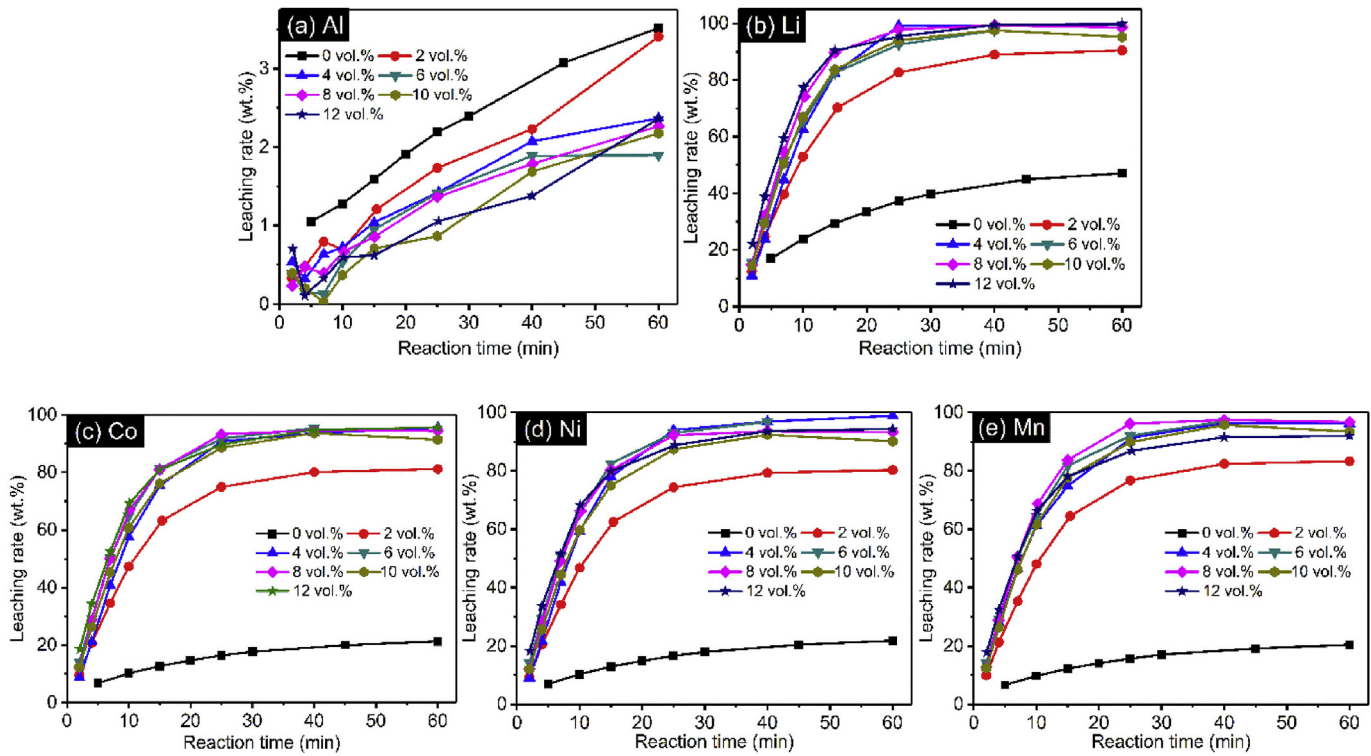


Fig. 5. Leaching rates of (a) Al, (b) Li, (c) Co, (d) Ni and (e) Mn from the cathode scrap under different H₂O₂ contents (acetic acid concentration of 3.5 mol/L, S/L ratio of 40 g/L at 60 °C for 0 min to 90 min).

Table 1

The summary of different leaching result for Ni, Co, Mn and/or Al based cathode materials.

Cathode material	Acid	Leaching rate (wt.%)	Reference
LiNi _{0.33} Co _{0.33} Mn _{0.33} O ₂	Lactic acid	Li 97.7%, Ni 98.2%, Co 98.9%, Mn 98.4%	(Li et al., 2017)
LiNi _{0.33} Co _{0.33} Mn _{0.33} O ₂	TFA	Li 68.9%, Ni 35.01%, Co 35.39%, Mn 35.18%, Al 9.31%	(Zhang et al., 2014)
LiNi _{0.33} Co _{0.33} Mn _{0.33} O ₂	TCA	Li 99.7%, Ni 93.0%, Co 91.8%, Mn 89.8%, Al 7.0%	(Zhang et al., 2015)
LiNi _{0.33} Co _{0.33} Mn _{0.33} O ₂	Formic acid	Li 99.3%, Ni 93.81%, Co 90.49%, Mn 88.66%, Al 2.24%	(Gao et al., 2017)
LiNi _{0.33} Co _{0.33} Mn _{0.33} O ₂	Citric acid	More than 98%	(Yao et al., 2015)
LiNi _{0.33} Co _{0.33} Mn _{0.33} O ₂	L-Tartaric acid	Li 98.64%, Ni 99.31%, Co 98.64%, Mn 99.31%	(He et al., 2017a)
LiNi _{0.33} Co _{0.33} Mn _{0.33} O ₂	Fruit juice	94-100%	(Pant and Dolker, 2017)
LiNi _{0.33} Co _{0.33} Mn _{0.33} O ₂	H ₂ SO ₄	Li 96.7%, Ni 96.4%, Co 91.6%, Mn 87.9%	(Meshram et al., 2015a)
LiNi _{0.33} Co _{0.33} Mn _{0.33} O ₂	H ₂ SO ₄	Li 93.4%, Ni 96.3%, Co 66.2%, Mn 50.2%	(Meshram et al., 2015b)
LiNi _{0.33} Co _{0.33} Mn _{0.33} O ₂	H ₂ SO ₄	Li, Ni, Co, Mn 99.7%	(He et al., 2017b)
LiNi _{0.8} Co _{0.15} Al _{0.05} O ₂	HCl	Li, Ni, Co, Al 100%	(Joulie et al., 2014)
Mixing cathode material	Citric acid	About Li 99%, Ni 91%, Co 92%, Mn 94%	(Chen et al., 2016)
Mixing cathode material	H ₂ SO ₄	Mn 97.8%, Ni 99.4%, Co 99.6%, Li 98.8%, Al 97.8%, Cu 64.7%	(Nayl et al., 2014)
Mixing cathode material	H ₂ SO ₄	Almost 100%	(Zou et al., 2013)
Mixing cathode material	H ₂ SO ₄	Co 37%, Cu 1%, Al 85%, Li 55%	(Mantuano et al., 2006)
Mixing cathode material	HCl	Co 99.5%, Li 99.9%, Ni 99.8%, Mn 99.8%	(Wang et al., 2009)
Mixing cathode material	HCl	Co, Mn > 99%	(Barik et al., 2017)
Mixing cathode material	HNO ₃	Li 100%	(Castillo et al., 2002)
Mixing cathode material	HNO ₃	Co 91%, Li 77%, Ni 99%, Mn 100%	(Guan et al., 2017)
Mixing cathode material	HCl	Ni >95%, Co 95%, Mn 95%	(Li et al., 2009)

$$\frac{X}{3k_M} + \frac{R_0}{6D_e} \left[1 - 3(1-X)^{\frac{2}{3}} + 2(1-X) \right] + \frac{1}{k_{rea}} \left[1 - (1-X)^{\frac{1}{3}} \right] = \frac{MC_0}{x\rho R_0} t \quad (6)$$

where k_M is the mass transfer coefficient in liquid boundary layer, X is the fraction reacted (i.e., leaching rate), R_0 is the radius of the particle, D_e is the mass transfer coefficient in the residue layer, k_{rea} is the reaction rate constant, M is the molar weight of the cathode material, t is the reaction time, C_0 is the acetic acid concentration at

$t=0$, ρ is the density of the cathode material, x is the electron transfer number in the reaction of (4) or (5).

For simplification, the leaching rate can be assumed to be controlled by the following kinetics models: liquid boundary layer mass transfer control model (Eq. (7)), surface chemical reaction control model (Eq. (8)) or residue layer diffusion control model (Eq. (9)).

$$X = k_1 \cdot t \quad (7)$$

$$1 - (1 - X)^{\frac{1}{3}} = k_2 \cdot t \quad (8)$$

$$1 - 3(1 - X)^{\frac{2}{3}} + 2(1 - X) = k_3 \cdot t \quad (9)$$

Where, k_1 , k_2 and k_3 are the slopes of the fitted lines, t is the reaction time (min).

Considering the leaching of metal values from the cathode scrap of LIBs can be promoted at the presence of reductant, it is necessary to analyze the leaching mechanisms with and without the addition of H_2O_2 in order to compare and study the quantitative influence of reductant on the leaching process.

3.2.1. Kinetics analysis without the addition of reductant

3.2.1.1. Selection of kinetics equation. Taking the leaching rates of Co from the cathode scrap of LIBs under different reaction temperatures in the absence of H_2O_2 as an example (Fig. 4), the above-mentioned kinetics models are applied and compared to find out the best kinetics equation. As indicated in Fig. 6, the residue layer diffusion control model (Eq. (9)) exhibits the best fitting relevance among the other kinetics models (Table S1).

Under the specific leaching conditions (the same acid concentration, S/L ratio and reductant content), the reaction rate constant of the leaching process can be described by the empirical Arrhenius law (Jha et al., 2013):

$$k = Ae^{\frac{-E_a}{RT}} \quad (10)$$

where R (J/mol·K) is the universal gas constant; A (1/min) is the pre-exponential factor; E_a (J/mol) is the apparent activation energy, and T (K) is the absolute temperature. As A is variable along with different leaching conditions, thus the kinetic equation during the leaching of metal values from the cathode scrap of LIBs can be described by Eq. (11) (Li et al., 2014) according to the vanadium leaching process.

$$k = k_0 C_{acetic\ acid}^M (S/L)^N e^{\frac{-E_a}{RT}} \quad (11)$$

where k_0 (1/min) is the pre-exponential factor; $C_{acetic\ acid}$ (mol/L) is the acetic acid concentration; M is the acid concentration index constant, S/L (g/L) is the S/L ratio; N is the S/L ratio index constant, R (J/mol·K) is the universal gas constant; E_a (J/mol) is the apparent activation energy; and T (K) is the absolute temperature. Converting the Eq. (11) into the form of Eq. (12), the kinetics parameters such as M , N , E_a and k_0 can be calculated under the specific experimental conditions.

$$\ln k = \ln k_0 + M \ln C_{acetic\ acid} + N \ln (S/L) - E_a/RT \quad (12)$$

3.2.1.2. Kinetics analysis under different acid concentrations. Based on the leaching rates under different acetic acid concentrations in the absence of H_2O_2 (Fig. 2), the plots of $1 - 3(1 - X)^{2/3} + 2(1 - X)$ vs. t could be drawn to determine k during the leaching of Co, Ni, Mn and Li from the cathode scrap. As shown in Fig. 7 and Table S2, they display a good linear relationship for Ni, Co, Mn and Li with almost the coefficients of determination (Adj, R^2) higher than 0.99.

According to the Eq. (12), the plot of $\ln k$ vs. $\ln C_{acetic\ acid}$ (Fig. S8) is a straight line with a slope of M if the S/L ratio and reaction temperature are constants, therefore the M values during the leaching of Co, Ni, Mn and Li from the cathode scrap (Table 2) are 0.8754, 0.8538, 0.8660 and 0.9439, respectively.

3.2.1.3. Kinetics analysis under different S/L ratios. Similar to the determination of M , the k values during the leaching of Co, Ni, Mn and Li from the cathode scrap under different S/L ratios (Fig. 3) can be determined by plotting $1 - 3(1 - X)^{2/3} + 2(1 - X)$ vs. t . As shown in Fig. 8 and Table S3, almost all of the curves show good liner relationship for Co, Ni, Mn and Li with R^2 higher than 0.99. The plots of $\ln k$ vs. $\ln S/L$ (Fig. S9) are straight lines, and the N values for leaching of Co, Ni, Mn and Li (Table 3) from the cathode scrap are -0.5139 , -0.5019 , -0.5006 , -0.5631 , respectively. Different from M values, the N value for each metal is a negative number revealing that the leaching rates of Ni, Co, Mn and Li decreased with the increase of S/L ratio. This finding is well in accordance with the results of leaching experiments (Fig. 3).

3.2.1.4. Kinetics analysis under different reaction temperatures. Based on the leaching rates provided in Fig. 4, plots of $1 - 3(1 - X)^{2/3} + 2(1 - X)$ vs. t during leaching of metal values from the cathode scrap under different reaction temperatures in the absence of H_2O_2 are presented in Fig. 9. It is indicated that these fitting lines show good liner relationship with the R^2 higher than 0.96 (Table S4). By plotting $\ln k$ vs. $1/T$, the E_a values for leaching of Co, Ni, Mn and Li can be determined from the slopes of the corresponding fitting lines (Fig. S10) with 54.22 kJ/mol, 53.21 kJ/mol, 55.68 kJ/mol and 52.04 kJ/mol, respectively (Table 4). It is observed that the E_a for leaching of Li is lower than those of Ni, Co and Mn. It can be inferred that the leaching of Li is easier than other metal values which is consistent with the experimental results presented in Fig. 4. The reason may be ascribed that the leaching of Li is independent of any redox reaction process.

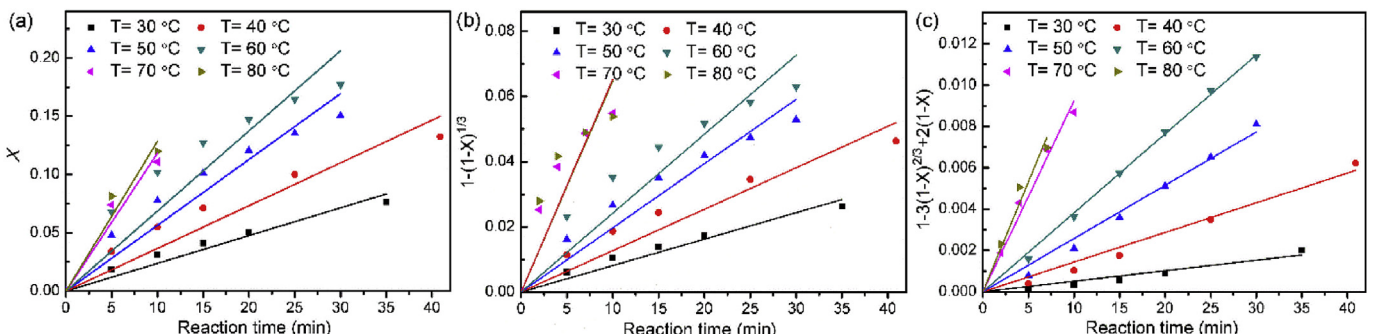


Fig. 6. Kinetics analysis during the leaching of Co from the cathode scrap under different reaction temperatures without the addition of H_2O_2 by X vs. t (a), $1 - (1 - X)^{\frac{2}{3}}$ vs. t (b) and $1 - 3(1 - X)^{\frac{2}{3}} + 2(1 - X)$ vs. t (c).

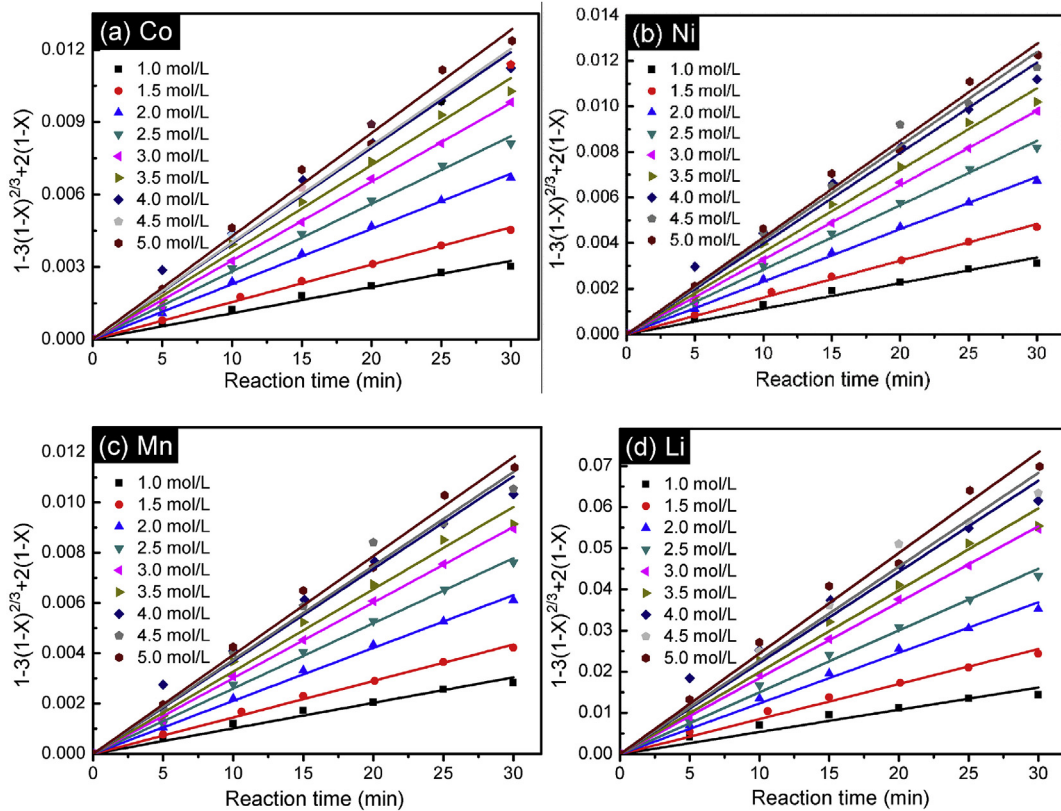


Fig. 7. Plots of $1 - 3(1-X)^{2/3} + 2(1-X)$ vs. t under different acetic concentrations in the absence of H_2O_2 : (a) Co, (b) Ni, (c) Mn and (d) Li.

Table 2

M values during the leaching of metal values from the cathode scrap in the absence of H_2O_2 using the residue layer diffusion control model.

Element	Slope	M	R^2
Co	0.8754	0.8754	0.9717
Ni	0.8538	0.8538	0.9760
Mn	0.8660	0.8660	0.9745
Li	0.9430	0.9439	0.9751

3.2.1.5. Determination of the kinetic equations. As shown in Eq. (11), the pre-exponential factor k_0 can be easily determined when the values of M, N, and E_a are available. Based on the kinetics parameters for leaching of metal values under various acetic acid concentrations with the experimental conditions of the S/L ratio of 40 g/L at 333.15 K for 30 min, the k_0 can be obtained (Table S5). Using the average k_0 values (Co: 2.67×10^5 /min, Ni: 1.81×10^5 /min, Mn: 3.99×10^5 /min, Li: 7.35×10^5 /min), the kinetic equations during the leaching of Co, Ni, Mn and Li under different acetic acid concentrations are given as follows:

$$\text{Co: } 1 - 3(1-X)^{\frac{2}{3}} + 2(1-X) = 2.67 \times 10^5 C_{\text{acetic acid}}^{0.8754} (S/L)^{-0.5139} e^{-\frac{5422}{RT}} \cdot t \quad (13)$$

$$\text{Ni: } 1 - 3(1-X)^{\frac{2}{3}} + 2(1-X) = 1.81 \times 10^5 C_{\text{acetic acid}}^{0.8538} (S/L)^{-0.5019} e^{-\frac{5321}{RT}} \cdot t \quad (14)$$

$$\text{Mn: } 1 - 3(1-X)^{\frac{2}{3}} + 2(1-X) = 3.99 \times 10^5 C_{\text{acetic acid}}^{0.8660} (S/L)^{-0.5006} e^{-\frac{5568}{RT}} \cdot t \quad (15)$$

$$\text{Li: } 1 - 3(1-X)^{\frac{2}{3}} + 2(1-X) = 7.35 \times 10^5 C_{\text{acetic acid}}^{0.9439} (S/L)^{-0.5631} e^{-\frac{5204}{RT}} \cdot t \quad (16)$$

The ranges of k_0 values for Co, Ni, Mn and Li are $(2.67 \pm 0.29) \times 10^5$ /min, $(1.81 \pm 0.19) \times 10^5$ /min, $(3.99 \pm 0.40) \times 10^5$ /min and $(7.35 \pm 1.10) \times 10^5$ /min, respectively. Since the absolute values of M and N for lithium are higher than other metal values, the acetic acid concentration and S/L ratio show more obvious influence on the leaching of Li than that of Co, Mn and Ni. With these kinetic equations, the leaching rates of metal values from the cathode scrap can be calculated under the specific acetic acid concentration, S/L ratio, reaction temperature and time, which may be helpful to adjust the leaching process in industrial application.

3.2.2. Kinetics analysis with the addition of reductant

Different from the situation in the absence of H_2O_2 , the introduction of H_2O_2 promote and accelerate the leaching speed of metal values from the cathode scrap which may alter the rate-limiting step and the corresponding kinetics behavior. Taking the leaching rates of Co under different reaction temperatures at the presence of H_2O_2 (Fig. S5), the three kinetics equations are applied in order to determine the most applicable equation. As shown in Table S6 and Fig. 10, the surface chemical reaction control model (Eq. (8)) displays the best fitting relevance. Similarly, the values of k during the leaching of metal values with the addition of H_2O_2 can also be

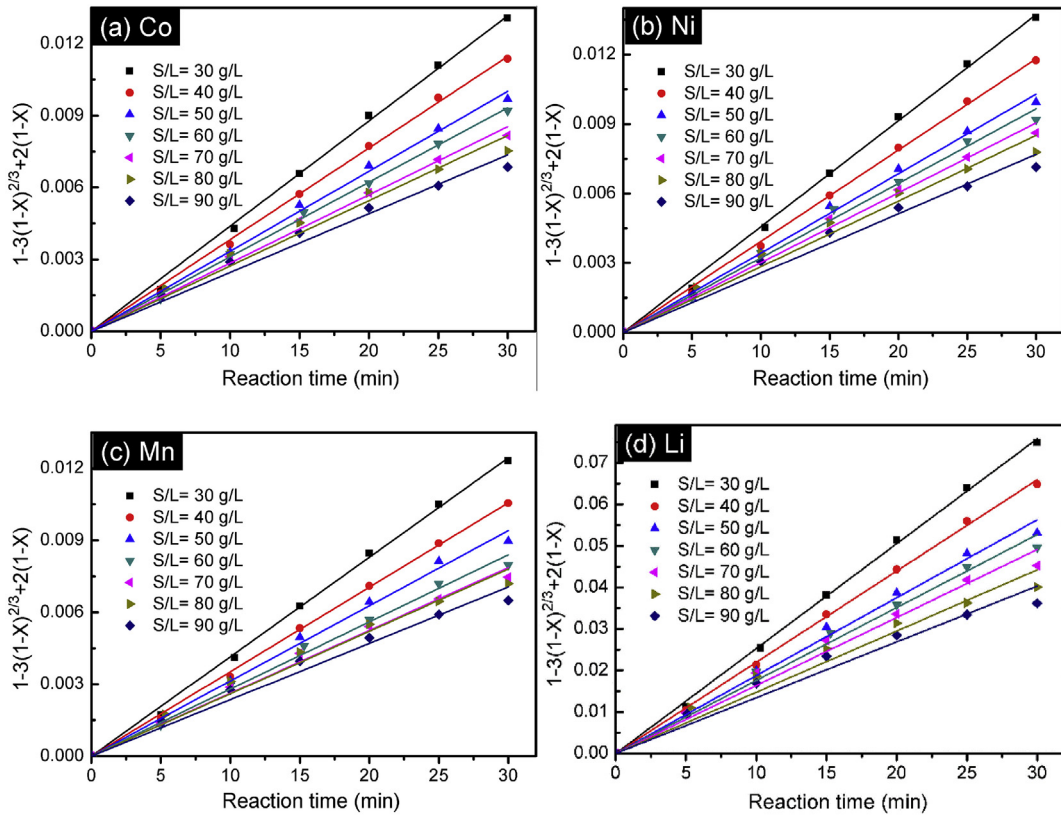


Fig. 8. Plots of $1-3(1-X)^{2/3}+2(1-X)$ vs. t under different S/L ratios in the absence of H_2O_2 : (a) Co, (b) Ni, (c) Mn and (d) Li.

Table 3
N values during the leaching of metal values from the cathode scrap in the absence of H_2O_2 using the residue layer diffusion control model.

Element	Slope	N	R^2
Co	-0.5139	-0.5139	0.9944
Ni	-0.5019	-0.5019	0.9907
Mn	-0.5006	-0.5006	0.9834
Li	-0.5631	-0.5631	0.9887

described by Eq. (11), and the Eq. (12) can be used to calculate the values of M, N and E_a .

Similar to the leaching process in the absence of H_2O_2 , the values of M and N can also be calculated by the same method during the leaching of metal values at the presence of H_2O_2 . According to the leaching rates of metal values presented in Fig. S6, the value of M during the leaching of Co, Ni, Mn and Li are calculated as 0.4415, 0.5576, 0.5951 and 0.7712, respectively (Figs. S11 and S12, Tables S7 and S8). Similarly, the value of N for Co, Ni, Mn and Li can also be determined as -0.7340, -0.8221, -0.8678 and -0.9534, respectively (Figs. S13 and S14, Tables S9 and S10) based on the leaching rates presented in Fig. S7. As shown in Fig. S16, there are distinct differences in the plots of $\ln k$ vs $1/T$ under the temperatures range from 30 °C to 80 °C. It is proved that the reaction temperature has insignificant effect on the leaching of metal values with the addition of H_2O_2 when the temperature is higher than 60 °C (Gao et al., 2017). The apparent activation energies during the leaching of Co, Ni, Mn and Li with the addition of H_2O_2 are 41.20 kJ/mol, 42.29 kJ/mol, 41.47 kJ/mol and 41.33 kJ/mol, respectively (Tables S11 and S12, Fig. S15).

To determine the kinetic equations, the pre-exponential factor k_0 for the leaching of metal values under different S/L ratios are calculated and the results are presented in Table S13. The values of

k_0 during the leaching of Co, Ni, Mn and Li are 1.23×10^8 /min, 2.51×10^8 /min, 7.40×10^7 /min and 6.47×10^7 /min, respectively, and the corresponding kinetic equations for the leaching of Co, Ni, Mn and Li are presented as follows:

$$\text{Co: } 1 - (1 - X)^{\frac{1}{3}} = 1.23 \times 10^8 C_{\text{acetic acid}}^{0.4415} (S/L)^{-0.7340} e^{-\frac{4120}{RT}} \cdot t \quad (17)$$

$$\text{Ni: } 1 - (1 - X)^{\frac{1}{3}} = 2.51 \times 10^8 C_{\text{acetic acid}}^{0.5576} (S/L)^{-0.8221} e^{-\frac{4229}{RT}} \cdot t \quad (18)$$

$$\text{Mn: } 1 - (1 - X)^{\frac{1}{3}} = 7.40 \times 10^7 C_{\text{acetic acid}}^{0.5951} (S/L)^{-0.8678} e^{-\frac{4147}{RT}} \cdot t \quad (19)$$

$$\text{Li: } 1 - (1 - X)^{\frac{1}{3}} = 6.47 \times 10^7 C_{\text{acetic acid}}^{0.7712} (S/L)^{-0.9534} e^{-\frac{4133}{RT}} \cdot t \quad (20)$$

The range of k_0 values for leaching of Co, Ni, Mn and Li are $(1.23 \pm 0.2) \times 10^8$ /min, $(2.51 \pm 1.05) \times 10^8$ /min, $(7.40 \pm 1.34) \times 10^7$ /min and $(6.47 \pm 1.43) \times 10^7$ /min, respectively. The tendency of the M, N, E_a is similar for leaching of metal values with and without the addition of reductant.

3.2.3. Discussion on the leaching kinetics

From the kinetic equations for leaching of metal values from the cathode scrap with and without the addition of H_2O_2 (Eq.(13)–(20)), the introduction of H_2O_2 transforms the leaching kinetic model from the residue layer diffusion control model to the surface chemical reaction control model. Before the addition of

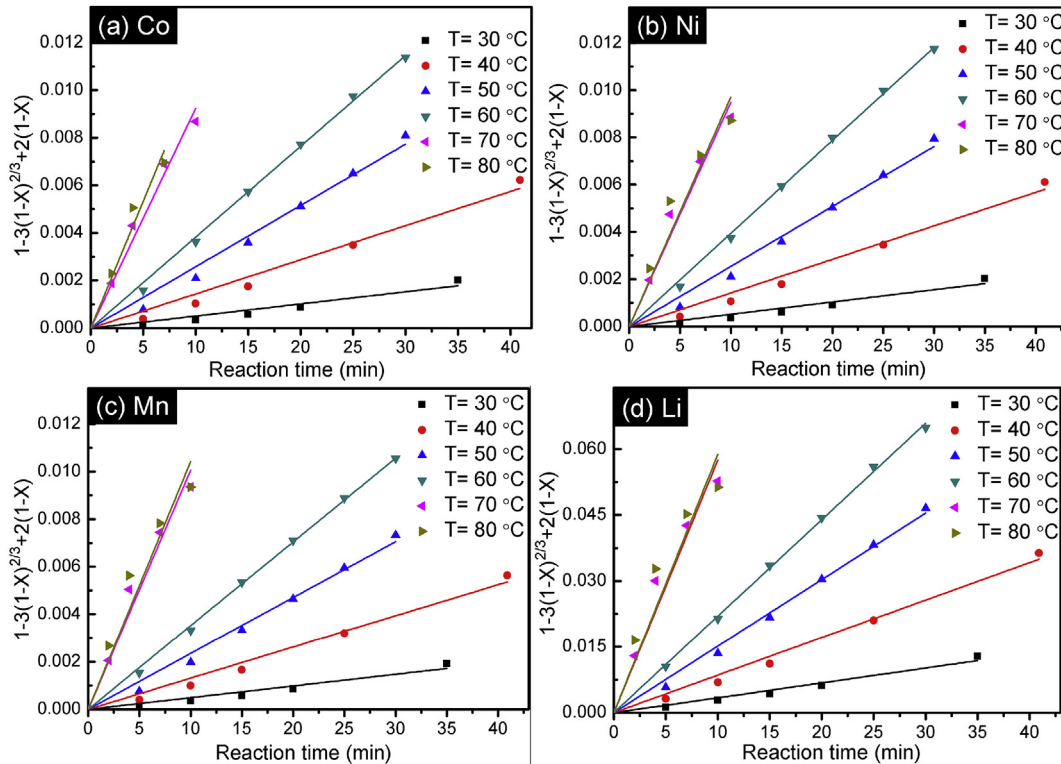


Fig. 9. Plots of $1-3(1-X)^{2/3}+2(1-X)$ vs. t under different reaction temperatures in the absence of H_2O_2 : (a) Co, (b) Ni, (c) Mn and (d) Li.

Table 4

E_a values during the leaching of metal values from the cathode scrap without H_2O_2 using the residue layer diffusion control model.

Element	Slope	E_a (kJ/mol)	R^2
Co	-6521.82	54.22	0.9698
Ni	-6399.91	53.21	0.9619
Mn	-6696.96	55.68	0.9630
Li	-6259.41	52.04	0.9627

reductant, the leaching speed is lower, compared to the situation at the presence of reductant. This is because higher valence metals in the $LiNi_{1/3}Co_{1/3}Mn_{1/3}O_2$ cathode material (Co^{3+} and Mn^{4+}) can't be easily leached into the leachate which will result in the formation of the residue layer and thus restraining the mass transfer. After the addition of reductant, the reaction speed of the leaching process is accelerated, and Co^{3+} and Mn^{4+} are reduced to the easily dissolved

Co^{2+} and Mn^{2+} efficiently. The gray residue layer, only including binder and acetylene black conductive agent, can form loose and porous structure in favor of accelerating the diffusion speed, and the leachant can easily react with the cathode material. Therefore, the rate-limiting step is transferred from the residue layer diffusion to surface chemical reaction after the introduction of reductant.

As indicated in Table 5, the value of k_0 increases, while the values of M and N decrease after the addition of reductant. As a result, the addition of reductant accelerates the leaching speed but weakens the influence of the acid concentration and S/L ratio on the leaching process. The decrease of apparent activation energy after the introduction of H_2O_2 means that the metal values in the cathode scrap is more easily leached out which is well agree with the experimental result.

Compared with the leaching residues in the absence of H_2O_2 (Fig. 11) at different leaching times under the optimal leaching conditions, the surface morphologies of the leaching residues in the

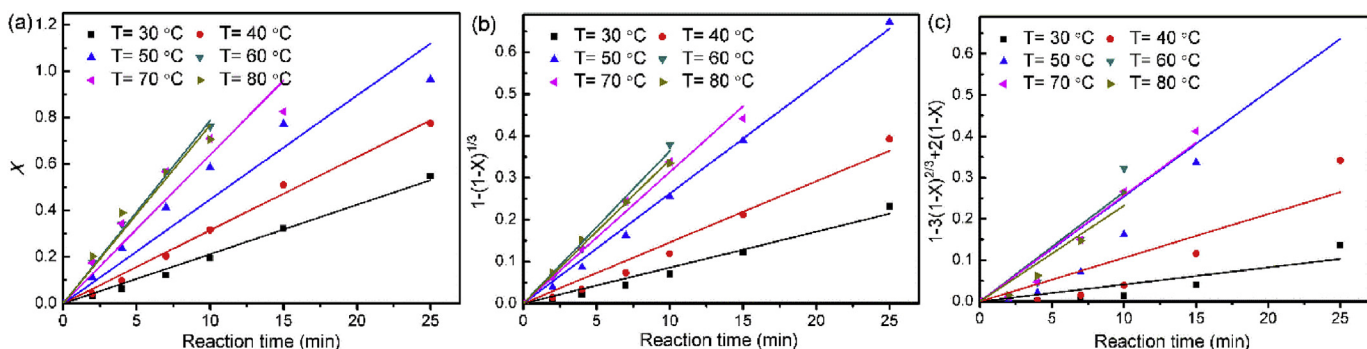


Fig. 10. Kinetics analysis during the leaching of Co from the cathode scrap under different reaction temperatures with the addition of H_2O_2 by X vs. t (a), $1-(1-X)^{1/3}$ vs. t (b) and $1-3(1-X)^{2/3}+2(1-X)$ vs. t (c).

Table 5

Values of k_0 , M, N and E_a during the leaching of metal values with and without the addition of H_2O_2 .

Element	k_0		M		N		$E_a(kJ/mol)$	
	Without H_2O_2	With H_2O_2	Without H_2O_2	With H_2O_2	Without H_2O_2	With H_2O_2	Without H_2O_2	With H_2O_2
Co	2.67×10^5	1.23×10^8	0.8754	0.4415	-0.5139	-0.7340	54.22	41.20
Ni	1.81×10^5	2.51×10^8	0.8538	0.5576	-0.5019	-0.8221	53.21	42.29
Mn	3.99×10^5	7.40×10^7	0.8660	0.5951	-0.5006	-0.8678	55.68	41.47
Li	7.35×10^5	6.47×10^7	0.9439	0.7712	-0.5631	-0.9534	52.04	41.33

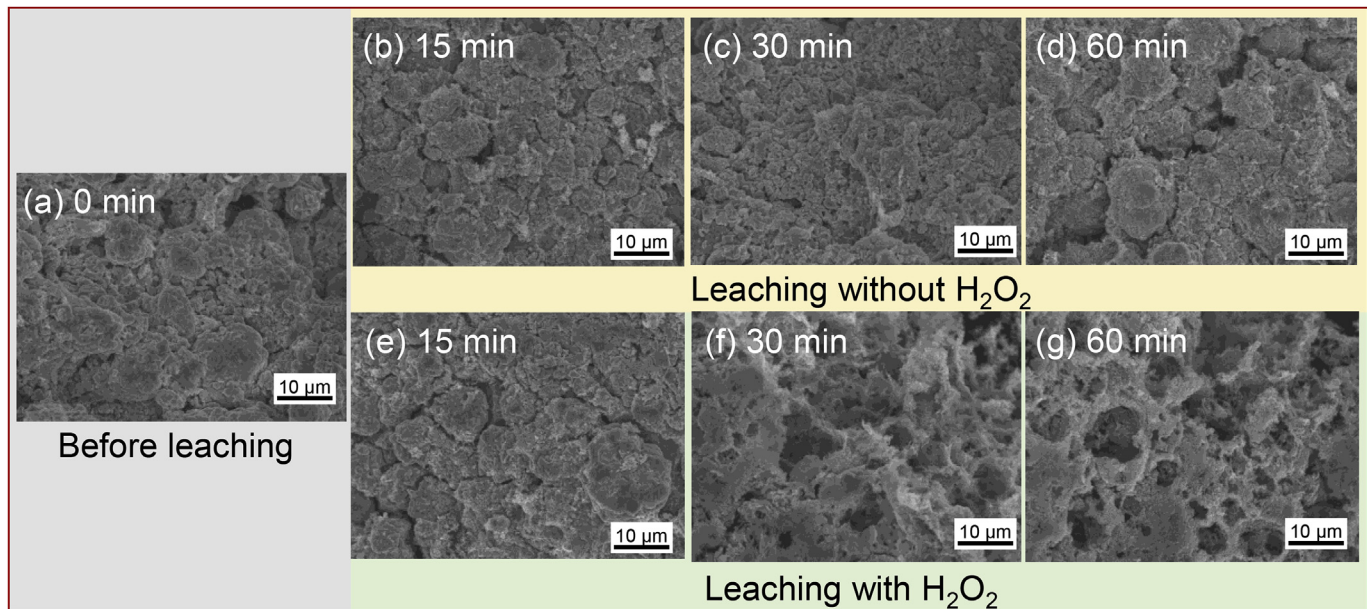


Fig. 11. SEM images of the leaching residues: (a) 0 min; without the addition of H_2O_2 at (b) 15 min, (c) 30 min and (d) 60 min; with the addition of H_2O_2 at (e) 15 min, (f) 30 min and (g) 60 min.

leaching with H_2O_2 vary obviously and demonstrate the loose and porous structures. According to Figs. 4 and 5, the leaching rates of Co, Mn and Ni are lower than 25 wt% during the leaching process in the absence of H_2O_2 while higher than 90 wt% at the presence of H_2O_2 . The leaching residues in the absence of H_2O_2 remain almost the same with the increase of the leaching time. Now that more than 90 wt% of Li, Co, Mn and Ni were leached into the solution, the leaching residues at the presence of H_2O_2 are gradually turned to "ash" layer consisting of conductive agent and binder with the increase of the leaching time. As shown in Fig. 11(g), there are plenty of pores with different sizes distributed in the leaching residues

after 60 min. The leachant and products can more easily diffuse through the loose and porous structures, so the rate-limiting step after the addition of H_2O_2 is transferred to the surface chemical reaction.

The XRD patterns of the cathode material and leaching residues with and without the addition of H_2O_2 are presented in Fig. 12. It is indicated that the crystal structures of the cathode material and the leaching residues in the absence of H_2O_2 are very similar with the regular α -NaFeO₂-type structure (Koyama et al., 2003). Although the leaching rate of Li is 44.86 wt% which is higher than those of other metals (Co: 19.99 wt%, Mn: 19.15 wt%, Ni: 20.44 wt%), the loss of Li doesn't change the crystal structure obviously. Since the metal values are almost leached into the solution completely at the presence of H_2O_2 (93.62 wt% of Co, 99.97 wt% of Li, 96.32 wt% of Mn and 92.67 wt% of Ni), thus there are only two obvious diffraction peaks left. The stronger diffraction peak can be indexed to the characteristic peak of the unreacted $LiNi_{1/3}Co_{1/3}Mn_{1/3}O_2$ particle, but the intensity is reduced drastically. Another diffraction peak is the characteristic peak of acetylene black (Ohzuku et al., 1993).

3.3. Development of a closed-loop recovery process for spent lithium-ion battery

According to the above experiments and analyses, a closed-loop process for recovering cathode scrap of LIBs based on acetic acid is developed and presented in Fig. 13. Dissembled from the spent LIBs or generated during the production of LIBs, the cathode scrap is selectively leached by acetic acid and H_2O_2 at the optimal leaching

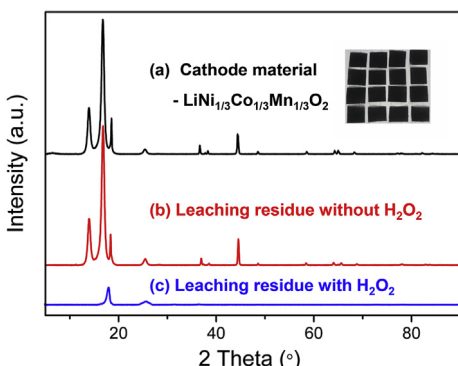


Fig. 12. XRD patterns of (a) cathode material-LiNi_{1/3}Co_{1/3}Mn_{1/3}O₂, (b) leaching residue without the addition of H_2O_2 , (c) leaching residue with the addition of H_2O_2 .

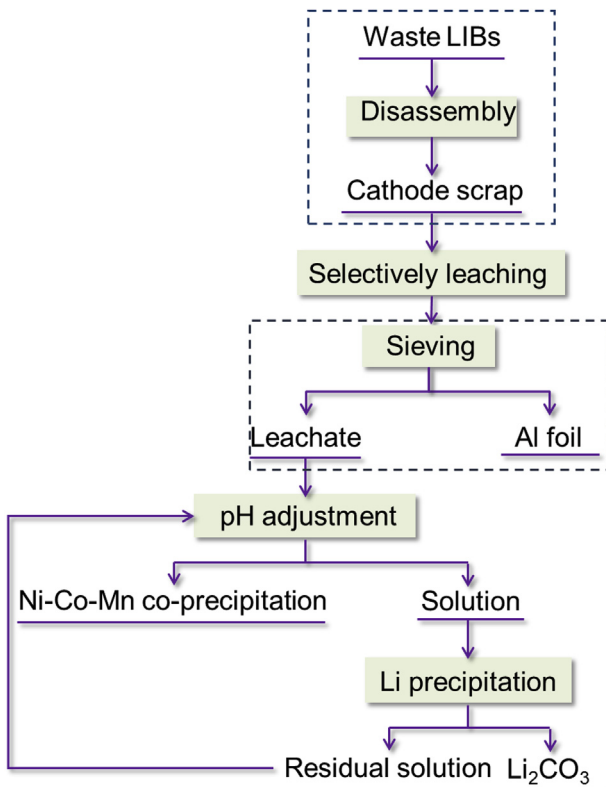


Fig. 13. Flowchart of the closed-loop recovery process for cathode scrap of LIBs based on acetic acid.

conditions. The high purity of Al foil can be obtained by sieving the leaching residues. By adjusting pH value and then adding Na_2CO_3 solution to the obtained leachate, the Ni, Co, Mn precursor and high purity of Li_2CO_3 can be synthesized. By process optimization, the purity of Li_2CO_3 can achieve 99.93(86)% (Table S14) which is higher than the earlier research (Gao et al., 2017). With this proposed recycling process, Al foil can be efficiently separated from the cathode scrap, while only 2.36 wt% of Al is leached into the leachate. Employing the small quantity of Al remained in the leachate as dopant, fresh cathode materials such as $\text{LiNi}_{1/3}\text{Co}_{1/3}\text{Mn}_{1/3}\text{O}_2$ with the improved rate performance and cycle stability may be resynthesized (Granata et al., 2012). This part of research is on the way and may be published later to make this research whole and systematic. With the products of high purity of Li_2CO_3 , Al foil, and Ni, Co, Mn co-precipitate, the metal values in the cathode scrap can be recovered as high value-added products with lower economic cost. By cycling the residual solution to pH adjustment process, the recovery rate of Li was increased and the global recovery rate of all metal values can achieve more than 90% as shown in Table S15.

4. Conclusions

A closed-loop process with improved leaching selectivity was developed to recover valuable metals from cathode scrap of spent LIBs. Lithium, cobalt, nickel and manganese could be selectively leached into solution using acetic acid while aluminum remained as its metallic form. The kinetics analysis was carried out to investigate the quantitative effect of reductant on the leaching process. The following conclusions can be drawn from this research: (1) A range of factors have been investigated in order to optimize the leaching process of cathode scrap in acetic acid

solution. Under the leaching conditions of 3.5 mol/L acetic acid, S/L ratio of 40 g/L at 60 °C and the H_2O_2 content of 4 vol%, the leaching rates of Co, Li, Mn and Ni can achieve 93.62 wt%, 99.97 wt% 96.32 wt % and 92.67 wt%, respectively within 60 min, while only 2.36 wt% of Al was leached out. (2) Based on the kinetics analysis, the quantitative effect of reductant on the leaching behavior of metal values from the cathode scrap was studied. It is indicated that the addition of reductant can alter the rate-controlling step from the residue layer diffusion to the surface chemical reaction during the leaching process. By calculating the parameters such as M, N, k_0 and E_a , the kinetic equations of each metal in the leaching process with and without reductant are determined. The introduction of reductant accelerates the leaching speed but decreases the influence of the acid concentration and S/L ratio. The decrease of apparent activation energy in the presence H_2O_2 makes the waste materials more easily react with the leachant. (3) Based on the leaching process, the high purity Li_2CO_3 (99.93(86)% can be recovered from spent lithium-ion battery. With the recovery efficiency of each metal higher than 90%, a closed-loop process was proposed and demonstrated for recovering cathode scrap with selectively leaching valuable metals based on acetic acid.

Acknowledgment

The authors acknowledge the financial support on this research from “1000 talents program” of China (Z.S.), the National Natural Science Foundation of China (No. 51425405), Beijing Science and Technology Program (No. Z171100002217028) and Project supported by Shanghai Cooperative Centre for WEEE Recycling (No. ZF1224). This research was also supported by the National Science – technology Support Plan Project (2015BAB02B05) and Project of China Postdoctoral Science Foundation for X. Zhang (No. 2016M591259).

Nomenclature

LIBs	Lithium ion batteries
S/L ratio	Solid to liquid ratio (g/L)
W	Metal values in cathode material (W=Ni, Co, Mn, Li, Al)
y	Leaching rate of metal values (W, wt.%)
t	Reaction time (min)
$C_{W,t}$	Concentration of metal W in the leachate under the leaching time t (W, g/L)
V	Volume of leachant (L)
m_W	The mass of metal W in the cathode scrap (W, g)
k_M	The mass transfer coefficient in liquid boundary layer
X	The fraction reacted (i.e., leaching rate)
R_0	The radius of the particle
D_e	Mass transfer coefficient in the residue layer
k_{rea}	Reaction rate constant
M	Molar weight of the cathode material
C_0	Acetic acid concentration at $t = 0$
ρ	Density of the cathode material
x	Electron transfer number in the reaction of (4) or (5)
k_1	The slope of the fitted lines for liquid boundary layer mass transfer control model
k_2	The slope of the fitted lines for surface chemical reaction control model
k_3	The slope of the fitted lines for residue layer diffusion control model
k	The reaction rate constant of the leaching process
R	The universal gas constant (J/mol·K)
A	Pre-exponential factor
E_a	Apparent activation energy (J/mol)

<i>T</i>	The absolute temperature (K)
<i>k₀</i>	Pre-exponential factor (1/min)
<i>C_{acetic acid}</i>	Acetic acid concentration (mol/L)
<i>M</i>	Acid concentration index constant
<i>N</i>	S/L ratio index constant

Appendix A. Supplementary data

Supplementary data related to this article can be found at <https://doi.org/10.1016/j.jclepro.2018.01.040>.

References

- Abdel-Aal, E.A., Rashad, M.M., 2004. Kinetic study on the leaching of spent nickel oxide catalyst with sulfuric acid. *Hydrometallurgy* 74, 189–194.
- Aydoğan, S., Aras, A., Uçar, G., Erdemoğlu, M., 2007. Dissolution kinetics of galena in acetic acid solutions with hydrogen peroxide. *Hydrometallurgy* 89, 189–195.
- Barik, S.P., Prabaharan, G., Kumar, L., 2017. Leaching and separation of Co and Mn from electrode materials of spent lithium-ion batteries using hydrochloric acid: laboratory and pilot scale study. *J. Clean. Prod.* 147, 37–43.
- Behera, S.S., Parhi, P.K., 2016. Leaching kinetics study of neodymium from the scrap magnet using acetic acid. *Separ. Purif. Technol.* 160, 59–66.
- Castillo, S., Ansart, F., Laberty-Robert, C., Portal, J., 2002. Advances in the recovering of spent lithium battery compounds. *J. Power Sources* 112, 247–254.
- Chen, X., Fan, B., Xu, L., Zhou, T., Kong, J., 2016. An atom-economic process for the recovery of high value-added metals from spent lithium-ion batteries. *J. Clean. Prod.* 112, 3562–3570.
- Dönmez, B., Demir, F., Laçın, O., 2009. Leaching kinetics of calcined magnesite in acetic acid solutions. *J. Ind. Eng. Chem.* 15, 865–869.
- Gao, W., Zhang, X., Zheng, X., Lin, X., Cao, H., Zhang, Y., Sun, Z., 2017. Lithium carbonate recovery from cathode scrap of spent lithium-ion battery: a closed-loop process. *Environ. Sci. Technol.* 51, 1662–1669.
- Granata, G., Moscardini, E., Pagnanelli, F., Trabucco, F., Toro, L., 2012. Product recovery from Li-ion battery wastes coming from an industrial pre-treatment plant: lab scale tests and process simulations. *J. Power Sources* 206, 393–401.
- Gratz, E., Sa, Q., Apelian, D., Wang, Y., 2014. A closed loop process for recycling spent lithium ion batteries. *J. Power Sources* 262, 255–262.
- Guan, J., Li, Y.G., Guo, Y.G., Su, R.J., Gao, G.L., Song, H.X., Yuan, H., Liang, B., Guo, Z.H., 2017. Mechanochemical process enhanced cobalt and lithium recycling from wasted lithium-ion batteries. *ACS Sustain. Chem. Eng.* 5, 1026–1032.
- Guo, Y., Li, F., Zhu, H., Li, G., Huang, J., He, W., 2015. Leaching lithium from the anode electrode materials of spent lithium-ion batteries by hydrochloric acid (HCl). *Waste Manag.* 51, 227–231.
- Hanisch, C., Loellhoeffel, T., Diekmann, J., Markley, K.J., Haselrieder, W., Kwade, A., 2015. Recycling of lithium-ion batteries: a novel method to separate coating and foil of electrodes. *J. Clean. Prod.* 108, 301–311.
- He, L.P., Sun, S.Y., Mu, Y.Y., Song, X.F., Yu, J.G., 2017a. Recovery of lithium, nickel, cobalt, and manganese from spent lithium-ion batteries using L-tartaric acid as a leachant. *ACS Sustain. Chem. Eng.* 5, 714–721.
- He, L.P., Sun, S.Y., Song, X.F., Yu, J.G., 2017b. Leaching process for recovering valuable metals from the LiNi₁/3Co₁/3Mn₁/3O₂ cathode of lithium-ion batteries. *Waste Manag.* 64, 171–181.
- Högönen, H.I., Kurama, H., 2012. Dissolution kinetics of magnesite waste in HCl solution. *Ind. Eng. Chem. Res.* 51, 1087–1092.
- Jha, M.K., Kumari, A., Jha, A.K., Kumar, V., Hait, J., Pandey, B.D., 2013. Recovery of lithium and cobalt from waste lithium ion batteries of mobile phone. *Waste Manag.* 33, 1890–1897.
- Joulie, M., Billy, E., Laucournet, R., Meyer, D., 2017. Current collectors as reducing agent to dissolve active materials of positive electrodes from Li-ion battery wastes. *Hydrometallurgy* 169, 426–432.
- Joulie, M., Laucournet, R., Billy, E., 2014. Hydrometallurgical process for the recovery of high value metals from spent lithium nickel cobalt aluminum oxide based lithium-ion batteries. *J. Power Sources* 247, 551–555.
- Khawam, A., Flanagan, D.R., 2006. Solid-state kinetic models: basics and mathematical fundamentals. *J. Phys. Chem.* 110, 17315–17328.
- Koyama, Y., Tanaka, I., Adachi, H., Makimura, Y., Ohzuku, T., 2003. Crystal and electronic structures of superstructural Li_{1-x}Co_{1/3}Ni_{1/3}Mn_{1/3}O₂ (0≤x≤1). *J. Power Sources* 119–121, 644–648.
- Li, G., Rao, M., Jiang, T., Huang, Q., Peng, Z., 2011. Leaching of limonitic laterite ore by acidic thiolsulfate solution. *Miner. Eng.* 24, 859–863.
- Li, J.H., Li, X.H., Hu, Q.Y., Wang, Z.X., Zheng, J.C., Wu, L., Zhang, L.X., 2009. Study of extraction and purification of Ni, Co and Mn from spent battery material. *Hydrometallurgy* 99, 7–12.
- Li, L., Fan, E.S., Guan, Y.B.A., Zhang, X.X., Xue, Q., Wei, L., Wu, F., Chen, R.J., 2017. Sustainable recovery of cathode materials from spent lithium-ion batteries using lactic acid leaching system. *ACS Sustain. Chem. Eng.* 5, 5224–5233.
- Li, L., Qu, W., Zhang, X., Lu, J., Chen, R., Wu, F., Amine, K., 2015. Succinic acid-based leaching system: a sustainable process for recovery of valuable metals from spent Li-ion batteries. *J. Power Sources* 282, 544–551.
- Li, Q., Liu, Z., Liu, Q., 2014. Kinetics of vanadium leaching from a spent industrial V205/TiO₂Catalyst by sulfuric acid. *Ind. Eng. Chem. Res.* 53, 2956–2962.
- Liu, Z.X., Yin, Z.L., Xiong, S.F., Chen, Y.G., Chen, Q.Y., 2014. Leaching and kinetic modeling of calcareous bornite in ammonia ammonium sulfate solution with sodium persulfate. *Hydrometallurgy* 144–145, 86–90.
- Mantuano, D.P., Dorella, G., Elias, R.C.A., Mansur, M.B., 2006. Analysis of a hydrometallurgical route to recover base metals from spent rechargeable batteries by liquid–liquid extraction with Cyanex 272. *J. Power Sources* 159, 1510–1518.
- Meshram, P., Pandey, B.D., Mankhand, T.R., 2015a. Hydrometallurgical processing of spent lithium ion batteries (LIBs) in the presence of a reducing agent with emphasis on kinetics of leaching. *Chem. Eng. J.* 281, 418–427.
- Meshram, P., Pandey, B.D., Mankhand, T.R., 2015b. Recovery of valuable metals from cathodic active material of spent lithium ion batteries: leaching and kinetic aspects. *Waste Manag.* 45, 306–313.
- Nayaka, G.P., Pai, K.V., Santhosh, G., Manjanna, J., 2016. Dissolution of cathode active material of spent Li-ion batteries using tartaric acid and ascorbic acid mixture to recover Co. *Hydrometallurgy* 161, 54–57.
- Nayil, A.A., Elkhashab, R.A., Badawy, S.M., El-Khateeb, M.A., 2014. Acid leaching of mixed spent Li-ion batteries. *Arab. J. Chem.* 10, S3632–S3639.
- Ohzuku, T., Ueda, A., Nagayama, M., Iwakoshi, Y., Komori, H., 1993. Comparative study of LiCoO₂, LiNi_{1/2}Co_{1/2}O₂ and LiNiO₂ for 4-volt secondary lithium cells. *Electrochim. Acta* 38, 1159–1167.
- Pagnanelli, F., Moscardini, E., Granata, G., Cerbelli, S., Agosta, L., Fieramosca, A., Toro, L., 2014. Acid reducing leaching of cathodic powder from spent lithium ion batteries: glucose oxidative pathways and particle area evolution. *J. Ind. Eng. Chem.* 20, 3201–3207.
- Pant, D., Dolker, T., 2017. Green and facile method for the recovery of spent Lithium Nickel Manganese Cobalt Oxide (NMC) based Lithium ion batteries. *Waste Manag.* 60, 689–695.
- Sa, Q., Gratz, E., He, M., Lu, W., Apelian, D., Wang, Y., 2015. Synthesis of high performance LiNi_{1/3}Mn_{1/3}Co_{1/3}O₂ from lithium ion battery recovery stream. *J. Power Sources* 282, 140–145.
- Shuva, M.A.H., Kurny, A.S.W., 2013. Dissolution kinetics of cathode of spent lithium ion battery in hydrochloric acid solutions. *J. Ins. Eng. India Series D* 94, 13–16.
- Sun, L., Qiu, K., 2012. Organic oxalate as leachant and precipitant for the recovery of valuable metals from spent lithium-ion batteries. *Waste Manag.* 32, 1575–1582.
- Sun, Z., Zhang, Y., Zheng, S.-L., Zhang, Y., 2009. A new method of potassium chromate production from chromite and KOH-KNO₃-H₂O binary submolten salt system. *AIChE J.* 55, 2646–2656.
- Wang, M.M., Zhang, C.C., Zhang, F.S., 2016. An environmental benign process for cobalt and lithium recovery from spent lithium-ion batteries by mechanochemical approach. *Waste Manag.* 51, 239–244.
- Wang, R.-C., Lin, Y.-C., Wu, S.-H., 2009. A novel recovery process of metal values from the cathode active materials of the lithium-ion secondary batteries. *Hydrometallurgy* 99, 194–201.
- Weng, Y., Xu, S., Huang, G., Jiang, C., 2013. Synthesis and performance of Li[(Ni_{1/3}Co_{1/3}Mn_{1/3})_{1-x}Mg_x]O₂ prepared from spent lithium ion batteries. *J. Hazard Mater.* 246–247, 163–172.
- Xin, Y., Guo, X., Chen, S., Wang, J., Wu, F., Xin, B., 2016. Bioleaching of valuable metals Li, Co, Ni and Mn from spent electric vehicle Li-ion batteries for the purpose of recovery. *J. Clean. Prod.* 116, 249–258.
- Yang, L., Xi, G., Xi, Y., 2015. Recovery of Co, Mn, Ni, and Li from spent lithium ion batteries for the preparation of LiNi_xCoyMn_zO₂ cathode materials. *Ceram. Int.* 41, 11498–11503.
- Yang, Z., Lu, J., Bian, D., Zhang, W., Yang, X., Xia, J., Chen, G., Gu, H., Ma, G., 2014. Stepwise co-precipitation to synthesize LiNi_{1/3}Co_{1/3}Mn_{1/3}O₂ one-dimensional hierarchical structure for lithium ion batteries. *J. Power Sources* 272, 144–151.
- Yao, L., Feng, Y., Xi, G., 2015. A new method for the synthesis of LiNi_{1/3}Co_{1/3}Mn_{1/3}O₂ from waste lithium ion batteries. *RSC Adv.* 5, 44107–44114.
- Yao, L., Yao, H.S., Xi, G.X., Feng, Y., 2016. Recycling and synthesis of LiNi_{1/3}Co_{1/3}Mn_{1/3}O₂ from waste lithium ion batteries using D,L-malic acid. *RSC Adv.* 6, 17947–17954.
- Zeng, X.L., Li, J.H., Singh, N., 2014. Recycling of spent lithium-ion battery: a critical review. *Critical reviews in environ. Sci. Technol.* 44, 1129–1165.
- Zhang, X., Cao, H., Xie, Y., Ning, P., An, H., You, H., Nawaz, F., 2015. A closed-loop process for recycling LiNi_{1/3}Co_{1/3}Mn_{1/3}O₂ from the cathode scraps of lithium-ion batteries: process optimization and kinetics analysis. *Separ. Purif. Technol.* 150, 186–195.
- Zhang, X., Xie, Y., Cao, H., Nawaz, F., Zhang, Y., 2014. A novel process for recycling and resynthesizing LiNi_{1/3}Co_{1/3}Mn_{1/3}O₂ from the cathode scraps intended for lithium-ion batteries. *Waste Manag.* 34, 1715–1724.
- Zheng, X., Gao, W., Zhang, X., He, M., Lin, X., Cao, H., Zhang, Y., Sun, Z., 2017. Spent lithium-ion battery recycling – reductive ammonia leaching of metals from cathode scrap by sodium sulphite. *Waste Manag.* 60, 680–688.
- Zhu, X., He, X., Yang, J., Gao, L., Liu, J., Yang, D., Sun, X., Zhang, W., Wang, Q., Kumar, R.V., 2013. Leaching of spent lead acid battery paste components by sodium citrate and acetic acid. *J. Hazard Mater.* 250–251, 387–396.
- Zou, H., Gratz, E., Apelian, D., Wang, Y., 2013. A novel method to recycle mixed cathode materials for lithium ion batteries. *Green Chem.* 15, 1183–1191.